We are IntechOpen,
the world's leading publisher of
Open Access books
Built by scientists, for scientists

6,900
Open access books available

186,000
International authors and editors

200M
Downloads

Our authors are among the

154
Countries delivered to

TOP 1%
most cited scientists

12.2%
Contributors from top 500 universities

BOOK CITATION INDEX
CLARIVATE ANALYTICS
INDEXED

WEB OF SCIENCE™

Selection of our books indexed in the Book Citation Index
in Web of Science™ Core Collection (BKCI)

Interested in publishing with us?
Contact book.department@intechopen.com

Structure and Dynamics of Plumes Generated by Small Rivers

Alexander Osadchiev and Peter Zavialov

Abstract

The total share of small rivers in the influxes of fluvial water and suspended matter to the world ocean is estimated at between 25 and 40%. On a regional scale, this contribution can be even more significant for many coastal regions. In this chapter, we show that dynamics of small river plumes is significantly different from that of plumes generated by large rivers. Spatial structure of small plumes is generally characterized by sharper horizontal and vertical gradients. As a result, small plumes exhibit more energetic temporal variability in response to external forcing. In this chapter, we address several dynamical features typical for small plumes. We describe and discuss the response of small plumes to wind forcing and river discharge variability, the interaction between neighboring small plumes, and the generation of high-frequency internal waves in coastal ocean by small rivers. We also substantiate the Lagrangian approach to numerical modeling of small river plumes.

Keywords: river plumes, small rivers, plume dynamics, wind forcing, plume interaction, internal waves, Lagrangian modeling

1. Introduction

River discharges inflow to sea and form buoyant river plumes at coastal areas in many world regions. The total surface area and volume of river plumes are relatively small as compared to the saline ambient sea. However, river plumes govern land-ocean fluxes of fluvial water, sediments, nutrients, and pollutants and, thus, significantly influence many physical, biological, and geochemical processes on the continental shelf [1–6]. Structure, dynamics, and variability of river plumes are key factors for understanding mechanisms of advection, convection, transformation, accumulation, and dissipation of fluvial discharge as well as suspended and dissolved river-borne constituents in the coastal sea [7–9].

Two groups of factors govern the processes of formation, spreading, and mixing of river plumes. Immanent characteristics of local landscapes, namely shoreline and sea bottom features, morphology of river mouths, and latitude, which define the local magnitude of the Coriolis force, define the first group of factors [10–13]. The second group consists of variable external forcing conditions, which include river discharge, local wind, coastal circulation, tides, waves, and stratification of the ambient ocean [14–21]. The structure and dynamics of a river plume also strongly depend on its spatial scale. Sizes of river plumes vary from meters to hundreds of kilometers due to large ranges of freshwater discharge rate among world river

systems. Also, spatial scales of many river plumes have large variability within a year caused by seasonal changes in river discharge rates. It results in diverse patterns of formation, spreading, and mixing of a river plume on intra-annual time scale [22–25].

General aspects of the structure and dynamics of river plumes as well as their regional features were addressed in many previous studies. Nevertheless, these works were mostly focused on large river plumes, while small rivers plumes received relatively little attention. This is presumably caused by small influence of individual small plumes on coastal sea as compared to large plumes. Also, most of the world's small rivers are not covered by regular hydrological and discharge measurements, which result in a lack of information about their runoff volume and variability [26, 27].

The total share of small rivers in the influxes of fluvial water and suspended sediments to the world ocean is estimated at about 25 and 40%, respectively [28, 29]. Furthermore, this contribution is much more significant on a regional scale for many coastal regions. Under certain terrain and climatic conditions, the cumulative discharge from small rivers can greatly increase in response to heavy rains and become comparable to or even exceed the runoff of large rivers [30–33]. Flash floods at small rivers caused by active precipitation events can strongly influence the land-ocean buoyancy fluxes, heat, terrigenous sediments, nutrients, and anthropogenic pollutants. Many studies showed that they can affect coastal dynamics of certain world regions [13, 28, 34–37].

In this chapter, we focus on specific features of structure and dynamics of small river plumes, which are not typical for large plumes. In Section 2, we address spatial structure and temporal variability of small river plumes and analyze general aspects of difference between small and large plumes. In Section 3, we describe the Lagrangian numerical model that was specifically designed for simulation of spreading and mixing of small river plumes and the associated transport of river-borne suspended matter. Section 4 provides description and analysis of several important dynamical features of small plumes including the response of small plumes to wind forcing and river discharge variability (Section 4.1), the interaction between neighboring small plumes (Section 4.2), and the generation of high-frequency internal waves in small plumes by river discharge (Section 4.3). The conclusions are given in Section 5.

2. Structure of small river plumes

The process of transformation of freshwater discharge as a result of its interaction with saline sea water can be considered and analyzed on different spatial and temporal scales. Initially, river discharge inflows to sea from a river mouth and forms a sub-mesoscale or mesoscale water mass commonly referred as a river plume, where salinity is significantly lower than of surrounding sea water. Buoyancy force plays an important role in spreading and mixing of this freshened water mass; therefore, dynamics of river plumes and ambient sea is different because of salinity differences. Thus, salinity is the main characteristic that is used to distinguish river plumes and sea water, i.e., define the mixing zone where river plume ends and sea water starts.

A river plume is generally formed by one or multiple distinct sources. Structure and dynamical characteristics within a river plume are strongly nonhomogenous. In particular, salinity and velocity field in vicinity of freshwater source/sources are significantly different as compared to outer parts of a plume [9, 16]. A river plume is spreading and mixing with adjacent sea water, which results in transformation of

a river plume, but also influences physical, biological, and geochemical characteristics of ambient sea. Strength and extent of this influence mainly depend on volume of freshwater discharge and varies from negligible impact of small plumes formed by rivers with low discharge rates on coastal sea [20, 24, 38] to formation of stable freshened water masses in the upper sea layer on wide coastal and shelf areas [11, 39–41]. The latter water masses, commonly referred as regions of freshwater influence (ROFI), are characterized by more homogenous structure, significantly as greater spatial scales and lower temporal variability, as compared to river plumes.

We regard river plumes as water masses formed as a result of transformation of freshwater discharge in coastal sea on diurnal to synoptic time scales, while ROFI reproduce transformation of freshwater discharge on seasonal to annual time scales. River plume embedded into ROFI reproduces a continuous process of transformation of freshwater discharge and, therefore, cannot be distinctly distinguished. On the other hand, river plumes and ROFI have strongly different thermohaline characteristics and dynamics. Therefore, interaction between river plumes and surrounding ROFI significantly influences spreading dynamics and mixing of river plumes on synoptic time scale [5, 25, 31–33].

In this chapter, we focus on small river plumes; therefore, we need to determine characteristic properties of small plumes to distinguish them from large plumes. We define small plumes as plumes that do not form ROFI; i.e., residence time of freshened water in a small river plume is equal to hours and days. Dissipation of freshened water as a result of mixing of a small plume with subjacent saline sea limitedly influence ambient sea and does not result in accumulation of freshwater in adjacent sea area. As a result, small plumes are characterized by sharp salinity and, therefore, density gradient at their boundaries with ambient sea. This density gradient hinders vertical energy transfer between a small plume and subjacent sea.

This feature strongly affects spreading dynamics of a small plume due to following reasons. First, the majority of wind energy transferred to sea remains in a small plume, because vertical momentum flux diminishes at density gradient between a plume and subjacent sea. Thus, wind stress is concentrated in a shallow freshened surface layer that causes higher motion velocity and more quick response of dynamics of a small plume to variability of wind forcing, as compared to ambient sea [42, 43]. Second, circulation of adjacent sea limitedly affects spreading dynamics of a small plume, because density gradient hinders upward momentum flux from subjacent sea to a small plume [44]. It results in wind-driven dynamics of small plumes, which is characterized by very energetic temporal variability of their positions, shapes, and areas [45–47]. Spreading pattern of a small plume can dramatically change during several hours that is regularly registered by in situ and satellite data. High temporal variability of small plumes and their small vertical sizes often result in large inhomogeneity of their horizontal structure.

3. Lagrangian modeling of small river plumes

An important role of buoyancy force and density gradients are key features of dynamics of small river plumes, which is substantially different from dynamics of ambient sea. Small plumes are characterized by sharp spatial gradients and high temporal variability, while ambient sea has more stable and homogenous structure. Thus, an Eulerian approach denoted by state equations for a fixed point of space is suitable for modeling of complex dependences and feedbacks of sea dynamics, but exhibits certain difficulties if applied for modeling of small plumes. On the other
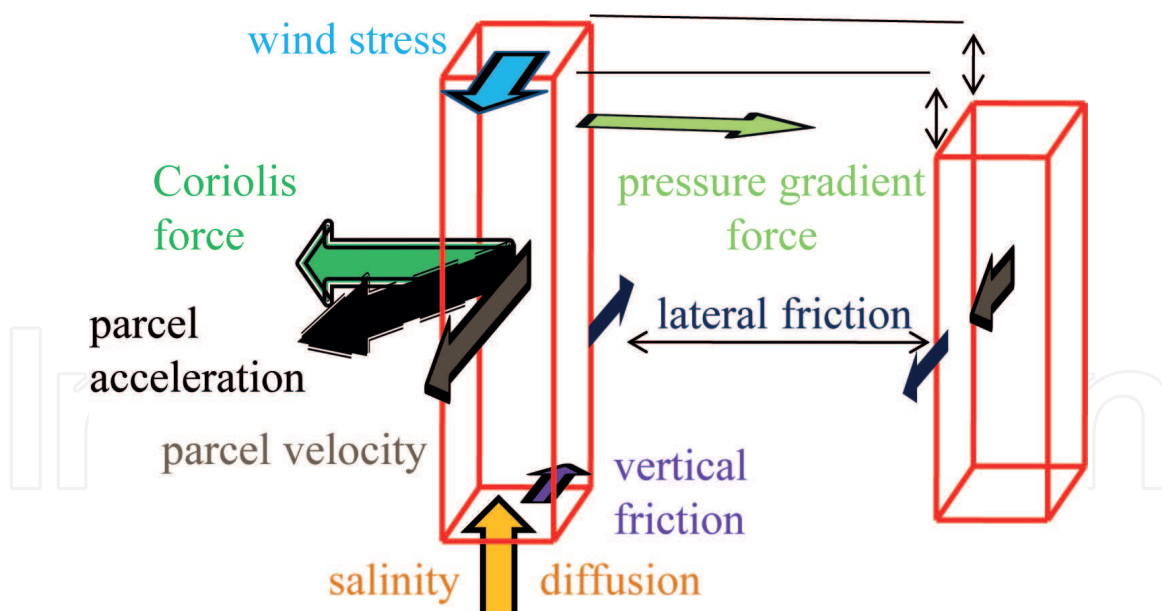
Figure 1.
Schematic of the forces applied to an individual parcel of a river plume.

hand, a Lagrangian approach denoted by state equations for a moving parcel of substance is more efficient for modeling of dynamically active processes and coherent structures typical for small plumes.

We developed a Lagrangian model called Surface-Trapped River Plume Evolution (STRiPE) for simulating the spreading of small river plumes and the associated transport of river-borne suspended sediments [45, 48]. STRiPE represents a river plume as a set of Lagrangian parcels or homogeneous water columns extending from the surface down to the boundary between the plume and the subjacent sea, while their horizontal sizes are presumed to be relatively small. These parcels are initially released from the river mouth and represent river runoff inflowing to sea. The subsequent motion of a parcel is determined by the momentum equation applied to this specific parcel. The overall set of parcels represents the river plume at every step of the model. Thus, the temporal evolution of the plume is simulated. We presume that the buoyant plume remains confined to the surface layer; therefore, the model describes the 2D motion of the parcels, although all parcels exhibit vertical mixing with subjacent sea water. Salinity and density of an individual parcel change in time until it eventually dissipates.

Motion equations, which are applied to an individual parcel, reproduce the main forces that determine river plume dynamics, namely, the Coriolis force, the pressure gradient force, the wind stress force, the friction at the lower boundary of the plume, and the lateral friction (**Figure 1**). At every step of the computation, the model reads the corresponding values from the input time series of river discharge rate, wind stress, and ambient sea current velocity data. Then, the model calculates the acceleration components (a_x, a_y) and the resulting velocity components (u, v) for the whole set of parcels. The STRiPE model tracks individual parcels and, therefore, does not use any spatial grid for solving the motion equations. However, an auxiliary horizontal grid with the respective increments Δx and Δy in zonal and meridional directions is used to calculate the spatial derivatives necessary for parameterizing the pressure gradient force and lateral friction applied to the parcel. Continuous fields of velocity, depth, and density within the plume are obtained by extrapolating the respective values from the overall set of parcels.

The momentum equations for an individual parcel are the following:

$$
\begin{aligned}
a_x^{i+1} = {}& fv_{x,y}^i + \frac{\tau_x^i}{\rho_{x,y}^i h_{x,y}^i} - \frac{\mu_v^i}{h_{x,y}^i} \frac{u_{x,y}^i - u_{sea}^i}{h_{x,y}^i} \\
& + \frac{\mu_h}{h_{x,y}^i} \left(\frac{\left(u_{x+\Delta x,y}^i - u_{x,y}^i\right) - \left(u_{x,y}^i - u_{x-\Delta x,y}^i\right)}{\Delta x} + \frac{\left(u_{x,y+\Delta y}^i - u_{x,y}^i\right) - \left(u_{x,y}^i - u_{x,y-\Delta y}^i\right)}{\Delta y} \right) \\
& - g \frac{h_{x+\Delta x,y}^i \rho_{x+\Delta x,y}^i \left(\rho_{sea} - \rho_{x+\Delta x,y}^i\right) - h_{x-\Delta x,y}^i \rho_{x-\Delta x,y}^i \left(\rho_{sea} - \rho_{x-\Delta x,y}^i\right)}{2\Delta x \rho_{sea} \rho_{x,y}^i}, \\
a_y^{i+1} = {}& -fu_{x,y}^i + \frac{\tau_y^i}{\rho_{x,y}^i h_{x,y}^i} - \frac{\mu_v^i}{h_{x,y}^i} \frac{v_{x,y}^i - v_{sea}^i}{h_{x,y}^i} \\
& + \frac{\mu_h}{h_{x,y}^i} \left(\frac{\left(v_{x+\Delta x,y}^i - v_{x,y}^i\right) - \left(v_{x,y}^i - v_{x-\Delta x,y}^i\right)}{\Delta x} + \frac{\left(v_{x,y+\Delta y}^i - v_{x,y}^i\right) - \left(v_{x,y}^i - v_{x,y-\Delta y}^i\right)}{\Delta y} \right) \\
& - g \frac{h_{x,y+\Delta y}^i \rho_{x,y+\Delta y}^i \left(\rho_{sea} - \rho_{x,y+\Delta y}^i\right) - h_{x,y-\Delta y}^i \rho_{x,y-\Delta y}^i \left(\rho_{sea} - \rho_{x,y-\Delta y}^i\right)}{2\Delta y \rho_{sea} \rho_{x,y}^i},
\end{aligned}
$$

$$(1)$$

where $(u_{x,y}, v_{x,y})$ are the interpolated velocity components at the (x, y) grid node, f is the Coriolis parameter, (τ_x, τ_y) are the wind stress components, ρ is the density of water in the parcel, h is the height of the parcel, $\rho_{x,y}$ is the interpolated density at the (x, y) grid node, $h_{x,y}$ is the interpolated height at the (x, y) grid node, μ_h, μ_v are the horizontal and vertical eddy viscosity coefficients, (u_{sea}, v_{sea}) are the ambient sea currents velocity components, ρ_{sea} is the ambient sea water density, and g is the gravity acceleration. The superscripts denote the model time steps. The first term in Eq. (1) denotes the Coriolis force, the second term stands for the wind stress, the third and fourth terms denote the bottom and lateral friction, and the fifth term stands for the pressure gradient force. After the acceleration components (a_x, a_y) are obtained from the momentum equations, the final velocities (u, v) for the period $(t, t + \Delta t)$ are calculated from kinematic formulas:

$$
\begin{aligned}
u^{i+1} &= u^i + a_x^{i+1}\Delta t, \\
v^{i+1} &= v^i + a_x^{i+1}\Delta t.
\end{aligned}
$$

$$(2)$$

In order to simulate the small-scale horizontal turbulent mixing, the deterministic approach described above was complemented by the random-walk Monte Carlo method [49]:

$$
\begin{aligned}
x^{i+1} &= x^i + u^{i+1}\Delta t - \frac{a_x^{i+1}\Delta t^2}{2} + \sqrt{2D_h^i \Delta t}\ \eta_x, \\
y^{i+1} &= y^i + v^{i+1}\Delta t - \frac{a_y^{i+1}\Delta t^2}{2} + \sqrt{2D_h^i \Delta t}\ \eta_y,
\end{aligned}
$$

$$(3)$$

where (x, y) are the coordinates of an individual parcel, Δt is the time step, D_h is the horizontal diffusion coefficient depending on the velocity field as specified below, and η_x, η_y are the independent random variables with standard normal

distribution. The horizontal diffusion coefficient used above was calculated from the Smagorinsky formula [50]:

$$D_h^i = \zeta_h \Delta x \Delta y \sqrt{ \left(\frac{u_{x+\Delta x, y}^i - u_{x-\Delta x, y}^i}{\Delta x} \right)^2 + \frac{1}{2} \left(\frac{v_{x+\Delta x, y}^i - v_{x-\Delta x, y}^i}{\Delta x} + \frac{u_{x, y+\Delta y}^i - u_{x, y-\Delta y}^i}{\Delta y} \right)^2 + \left(\frac{v_{x, y+\Delta y}^i - v_{x, y-\Delta y}^i}{\Delta y} \right)^2 },$$

where ζ_h is the scaling coefficient.

The simulation of the vertical dissipation of a plume parcel is based on the salinity diffusion equation and assumption that density depends linearly on salinity:

$$\frac{\partial \rho}{\partial t} = D_v \frac{\partial^2 S}{\partial z^2}, \tag{4}$$

or, in a discrete form,

$$\rho^{i+1} = \rho^i + \frac{D_v^i}{h_t} \frac{\rho_{sea} - \rho^i}{h^i} \Delta t. \tag{5}$$

where D_v is the vertical diffusion coefficient and h_t is the vertical turbulence scale. Hence, as the saline water from the subjacent sea is entrained into the plume gradually replacing the freshwater, the density of water in the parcel increases, while its height decreases according to the following linear equation:

$$\frac{\partial h}{\partial t} = -\frac{D_v^i}{h_t}, \tag{6}$$

or, in a discrete form,

$$h^{i+1} = h^i - \frac{D_v^i}{h_t} \Delta t. \tag{7}$$

The vertical diffusion coefficient divided by the vertical turbulence scale used above was calculated using the following parameterization based on Richardson number [51]:

$$\frac{D_v^i}{h_t} = \zeta_v \mu_v^i \left(1 - \min\left(1, Ri^i\right)^2 \right)^3, \tag{8}$$

where ζ_v is the scaling coefficient, $Ri^i = \frac{N^{i2}}{S^{i2}}$ is the Richardson number, $N^i = \sqrt{\frac{g}{\rho^i} \frac{\rho_{sea} - \rho^i}{h^i}}$ is the buoyancy frequency, and $S^i = \frac{\sqrt{\left(u^i - u_{sea}^i\right)^2 + \left(v^i - v_{sea}^i\right)^2}}{h^i}$ is the vertical shear.

Transport and settling of fine suspended sediments discharged from the river mouth is also simulated by STRiPE. In horizontal direction, sediment particle is defined as a passive tracer of a river plume; i.e., the horizontal movement of a

sediment particle is defined by velocity fields calculated within a plume at every modeling step. Vertical movement is calculated individually for every sediment fraction, which have different sizes of particles. For this purpose, we use a combination of a deterministic component defined by sinking of a particle under the gravity force and a stochastic random-walk scheme that reproduces influence of small-scale turbulent mixing. Sediment particles are initially released from the river mouth with river water. During its motion, a particle sinks within the river plume until it reaches the mixing zone between the river plume and the subjacent sea water. After the particle descends beneath the lower boundary of the plume, it is regarded as settled to ambient sea and is stopped to be simulated by STRiPE. The STRiPE is intended to simulate transport of relatively small particles with diameter less than 10^{-4} m; therefore, gravity-induced vertical motion is determined by Stokes' law, and particle settling velocity w_s is calculated as follows: $w_s = \frac{gd^2(\rho_s - \rho^i)}{18\mu\rho^i}$, where d is the sediment particle diameter, ρ_s is the sediment particle density, and μ is the dynamic water viscosity.

The total vertical displacement of a sediment particle determined by gravitational sinking, vertical advection, and turbulent mixing was parameterized by the random-walk Monte Carlo method, which represents features of spatially nonuniform turbulent mixing:

$$\Delta z = \left(w_s + \frac{\partial K}{\partial z}\right)\Delta t + \sqrt{\frac{2}{3}K_v\left(z + \frac{1}{2}\frac{\partial K_v}{\partial z}\Delta t\right)\Delta t}\,\eta, \qquad (9)$$

where Δz is the vertical displacement of a particle, K_v is the vertical diffusion coefficient, and η is a random process with standard normal distribution.

The main advantage of STRiPE lies in its computational efficiency in simulating spreading and mixing of river plumes as compared to Eulerian models. However, STRiPE does not reproduce any influence of a river plume on the ambient ocean, which is an important issue for large river plumes. Thus, STRiPE should be applied for simulation of spreading and mixing of small river plumes that limitedly influence the ambient sea.

4. Dynamics of small river plumes

In this section, we address dynamical features of small river plumes using the case study of the Mzymta plume and other small river plumes formed along the Russian coast of the Black Sea (RCBS) between the city of Novorossiysk and the city of Sochi (**Figure 2**). The drainage basin of RCBS is a narrow area (10–40 km wide) limited by the Greater Caucasus range at the east and the sea coast at the west. Steep gorges of this range form the drainage basins of several dozens of rivers that discharge to the sea at RCBS. Watershed basin areas of these rivers are relatively small, and the total freshwater runoff from the study region to the sea is estimated as 7 km^3 in a year [52].

Multiple buoyant plumes are formed along the coast of the study area. The largest plume is generally formed by the Mzymta River, which is the largest river of RCBS with mean monthly discharge equal to 20–120 m^3/s. The area of the Mzymta does not exceed 10 km^2 under average climatic discharge conditions. However, it can increase up to 50 km^2 during spring and summer freshet periods. Areas of the other river plumes of RCBS are even smaller except for rain-induced flash flooding
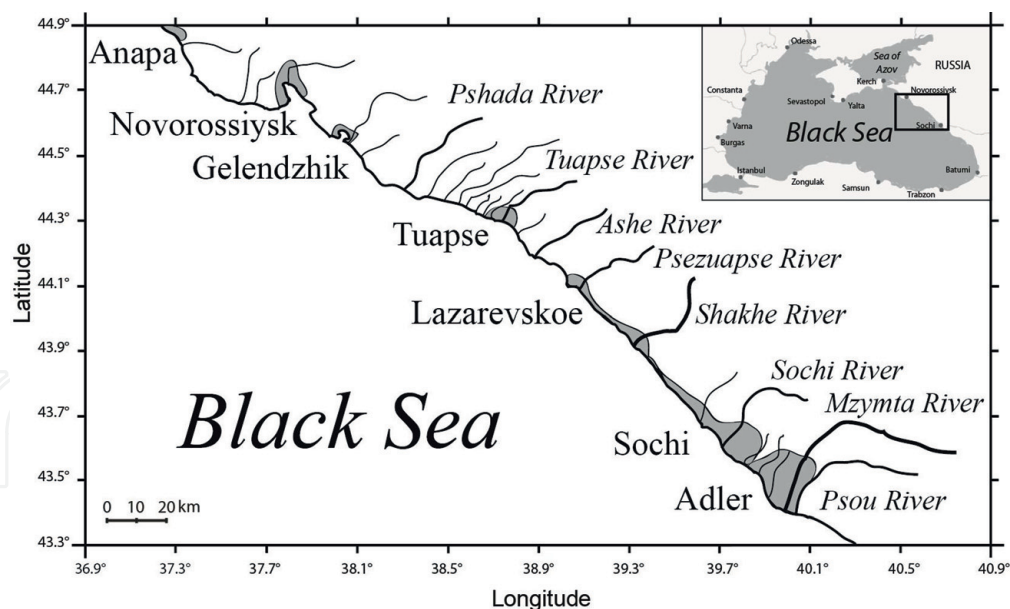
Figure 2.
Location of the largest rivers and cities of the Russian coast of the Black Sea.

periods. The rivers of the study region are significantly more turbid, as compared to sea water, due to elevated concentrations of terrigenous suspended sediments. As a result, surface salinity and turbidity show good correlation within the river plumes. Thus, optical satellite imagery can be effectively used to detect river plumes of RCBS [45, 46]. Both in situ and satellite measurements revealed high spatial and temporal variability of the river plumes of RCBS. Their areas, positions, and shapes can significantly change during several hours in response to variations of river discharge and local wind forcing [42, 43, 45].

4.1 Wind forcing and small river plumes

We used near-simultaneous ocean-color satellite imagery from NASA's Landsat 8 and ESA's Sentinel-2 missions to reconstruct surface currents along RCBS and study spreading dynamics of small river plumes formed in this area [53]. Several times a year, Landsat 8 and Sentinel-2 satellites both pass over the study area within a time interval of less than 10 minutes. The obtained near-simultaneous ocean-color composites can be used to reconstruct surface sea currents. In particular, they can be applied for detection of motion of frontal zones of river plumes, which are visible in optical satellite images. We used an optical flow algorithm applied to near-simultaneous Landsat 8 and Sentinel-2 images to reconstruct surface currents within the Mzymta plume. The obtained results reveal significant differences in wind-driven dynamics of the Mzymta plume and large plumes [12, 16, 54–58].

The main features of the dynamics of the Mzymta plume reconstructed from the satellite imagery are the following. First, the near-field part of the Mzymta plume is smaller than it is estimated by relevant parameterizations based on river discharge parameters designed for large plumes. Second, under low-wind-forcing conditions, the mid-field plume, i.e., a recirculating bulge adjacent to the river mouth, is not formed. The near-field freshwater jet directly transitions to the far-field part of the plume near the Mzymta mouth. Finally, during upwelling, onshore, and offshore wind-forcing periods, the wind-induced Ekman transport within the Mzymta plume occurs at a wide range of angles to the wind direction. It changes from values of 60–80° near the Mzymta mouth to 30–40° at the far-field part of the plume.

We presume the following physical interpretation of dynamical features of a small plume described above. The Mzymta River has a rapid flow (1–2 m/s), but is relatively shallow (1–1.5 m) in its mouth. Thus, relatively small volume of fresh water inflows to sea from the Mzymta River mouth at a relatively high speed. This jet is then abruptly decelerated by the vertical friction with the subjacent sea and the initial inertia of the jet decays in vicinity of the river mouth. Thus, according to the reconstructed surface velocity fields, size of the inertia-governed near-field part of the Mzymta plume is relatively small (1–2 km). It is of one order of magnitude less than, first, was reported by in situ measurements for river plumes formed by rivers with similar discharge rates but lower river inflow velocities [24, 38, 59, 60], and, second, theoretical values of near-field part of a plume numerically estimated by formulae described by [12, 54].

The near-field jet abruptly decelerates and forms a sharp pressure gradient in vicinity of the river mouth, which is directed seaward. As a result, anticyclonic recirculation flow directed to the river mouth is hindered by the pressure gradient force. Thus, the large river inflow velocity and low river discharge volume are the limiting factors for formation of an anticyclonic bulge under low wind-forcing conditions. On the other hand, in case of low velocity and/or a large volume of river inflow, it is not abruptly decelerated in vicinity of the river mouth, and strong velocity and pressure gradients are not formed.

Strong nonuniformity of motion patterns of different parts of the far-field plume in response to wind forcing are revealed by the reconstructed surface velocity fields. Upwelling, onshore, and offshore winds induce spreading of the most stratified parts of the plume adjacent to the Mzymta mouth at an angle of up to 80° to the direction of wind forcing. On the other hand, this angle diminishes to 30–40° at the less stratified outer parts of the plume. This effect is presumed to be caused by inhomogeneity of Ekman layer depth due to strong variability of stratification of the Mzymta plume. These results are supported by numerical experiments focused on relation between parameters of Ekman transport and river plume stratification [61].

Dynamical features of the Mzymta plume described above significantly influence its structure, spreading patterns, and the associated transport of suspended and dissolved river-borne constituents. First, freshwater discharge does not accumulate at the small near-field part of the Mzymta plume, which is not the case for large rivers [9, 15, 55]. As a result, freshwater discharge is mainly accumulated at the far-field part of the Mzymta plume. Winds cause spreading of a far-field plume along the direction of Ekman transport till it is limited by a coastline. Thus, location of a restraining coastline defines two stable states of a plume, which are generally indicated by downstream/upstream location of a sharp plume front. First, an alongshore downstream current is formed if spreading of a small plume is limited by a downstream coastline. Second, a small plume is arrested near its estuary if its spreading is restrained by an upstream coastline.

The observed large angles between surface flow and wind-forcing directions at the strongly stratified part of the Mzymta plume causes significantly different wind-govern spreading patterns of a small plume, as compared to large plumes (**Figure 3**). Upstream spreading of large river plumes is caused by upwelling wind forcing [22, 62, 63], while upstream spreading and accumulation of a small plume was observed only during onshore winds. On the opposite, upwelling wind forcing induced intense offshore spreading of a small plume, while largest cross-shore scales of large plumes were registered during offshore wind-forcing conditions [64, 65]. Downstream spreading of a small plume as an alongshore coastal current during downwelling wind-forcing conditions is similar to spreading patterns observed for large plumes [22, 62, 66–68].

4.2 Interaction between small river plumes

The Mzymta River has a drought period from late summer to the end of winter and a freshet period in spring and early summer caused by snow melting. All other rivers of the study region are mainly rain-fed and are prone to regular flash floods that provide the majority of their total annual runoff. These flash floods are characterized by sharp rises and falls of discharge due to small sizes (<900 km^2) and steep relief of the drainage basins and their high drainage densities (0.85–1.05). It results in quick response of discharge of these rivers on precipitation events, which can significantly increase during several hours after a heavy rain [69].

Under average climatic discharge conditions, plumes formed by small rivers at RCBS are distinctly separated because their spatial scales do not exceed the distances between the river estuaries. However, during rain-induced floods, the areas of the river plumes significantly increase, and the plumes can collide and coalesce with neighboring plumes (**Figure 4**). As a result, the point-source spread of continental discharge dominated by several large rivers under average climatic conditions can change to the line-source discharge from numerous small rivers situated along the coast in response to heavy rains. We studied interaction between these river plumes using a nested combination of the INMOM [70, 71] and the STRiPE numerical models [25]. The Eulerian model INMOM reproduced general ocean
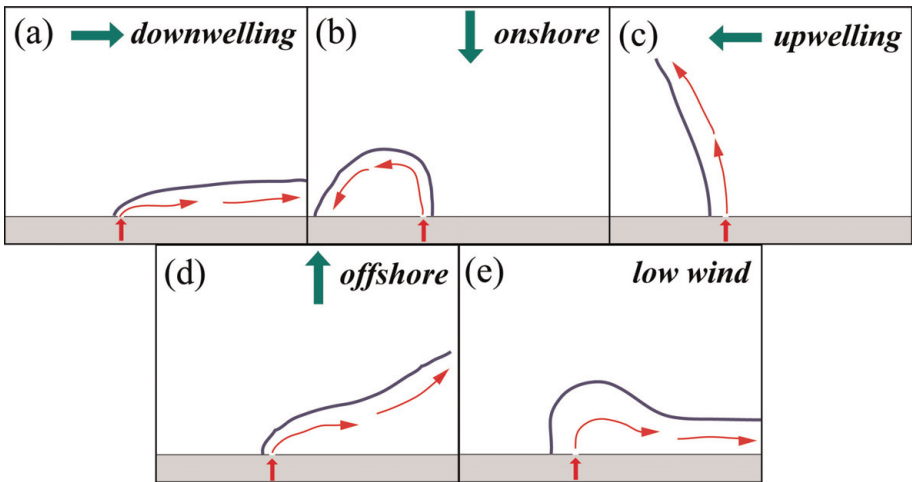

Figure 3.
Schematic of spreading patterns of a small river plume and the related locations of sharp frontal zones of a plume under (a) downwelling, (b) onshore, (c) upwelling, (d) offshore, and (e) low wind-forcing conditions.
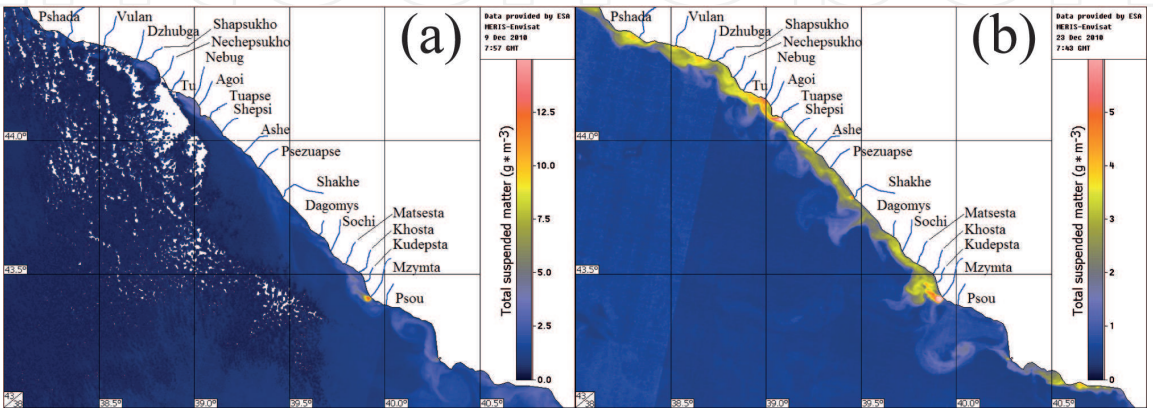

Figure 4.
Satellite-derived surface TSM distribution at the Russian coast of the Black Sea before (a) and after (b) a heavy rain, illustrating collision and coalescence of multiple small plumes at RCBS in response to rain-induced flooding event.

circulation at the northeastern part of the Black Sea and provided boundary conditions for the Lagrangian model STRiPE, which was used for simulating the dynamics of river plumes.

Numerical experiments showed that short-term rain-induced flooding events significantly influence sediment transport and deposition patterns at RCBS. Under average climatic discharge conditions, the total runoff of fluvial water and terrigenous sediments in the study area is dominated by several largest rivers. Discharge of fresh water and terrigenous sediments from the small rivers is relatively low. As a result, plumes formed by small rivers have small sizes, small water residence time, and their influence on coastal sea is almost negligible. Thus, river discharges affect local water quality and sediment accumulation only near the estuaries of several largest rivers. Heavy rains can induce a rapid and substantial increase in discharge of fresh water and terrigenous sediments from the small rivers of the study region. During these flash flooding periods, areas of small plumes substantially increase, neighboring plumes coalesce, and strips of freshened water masses can be formed along large segments of the seashore.

Numerical modeling revealed that interaction between river plumes significantly influence their structure and dynamics. During flash flooding periods, alongshore strips of freshened and turbid water are formed in the study region and their total length can exceed 200 km. The resulting line-source discharge pattern induces switch in dynamics of river plumes and transport pathways of river-borne suspended and dissolved matters at RCBS. The mixing intensity between the plumes and the adjacent strips of freshened and turbid water is relatively low due to the decrease of salinity gradient. As a result, the river plumes exhibit slower dissipation, have larger spatial scales, and have larger water residence time, as compared to point-source discharge conditions. Moreover, line-source discharge conditions induce alongshore geostrophic currents of turbid and freshened water. These currents induce the intense alongshore transport of river-borne sediments in a northwestern direction. This process strongly affects local water quality and causes active sediment accumulation along large segments of the sea shore at the study region, as compared to point-source discharge conditions.

4.3 Generation of high-frequency internal waves

High-frequency internal waves propagating offshore in small river plumes are regularly observed in satellite imagery in many world regions. In particular, Landsat 8 and Sentinel-2 ocean-color composites regularly reveal surface expressions of high-frequency internal waves propagating in small river plumes of RCBS [72]. Sources of these internal waves are small areas (100–200 m long and 25–100 m wide) adjacent to river mouths and elongated in directions of river inflows (**Figure 5a**). These waves propagate offshore from their source areas, and their surface expressions are distinctly observed at optical satellite imagery only within river plumes. These waves dissipate within river plumes at a distance of order of several kilometers from the river mouths or at lateral boundaries of river plumes, if size of a river plume is less than the decay distance of the internal waves. Ranges of wavelengths, phase speeds, and periods of internal waves reconstructed at multiple river plumes of the study region using satellite imagery are equal to 30–60 m, 0.45–0.65 m/s, and 65–90 s, respectively.

We presume the following mechanism of generation of internal waves described above by discharges of small and rapid rivers (**Figure 5b**). Velocity of a river runoff is of one order of magnitude higher than velocity of coastal circulation. It causes abrupt deceleration of a freshened flow, increase of its depth, and formation of a hydraulic jump. The resulting switch of flow conditions from supercritical to
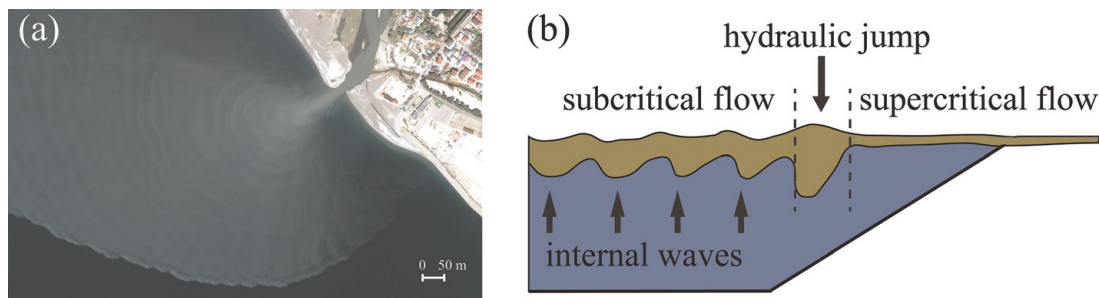
Figure 5.
WorldView-3 ocean color composite of the Mzymta plume from April 4, 2017 illustrating the formation and propagation of internal waves with high spatial resolution (a). Schematic of formation of a hydraulic jump and generation of internal waves by river discharge (b).

subcritical state causes generation of high-frequency internal waves. These waves propagate offshore in a stratified layer between the river plume and the subjacent saline sea. If the internal waves reach lateral boundary of a river plume, they abruptly dissipate due to relatively low stratification in the ambient sea. Thus, energy of internal waves is transformed to turbulence and increase mixing between the river plume and the subjacent sea.

A hydraulic jump described above is formed by river runoff under certain conditions that depend on properties of a river flow, ambient sea water, and a local topography. First, a supercritical freshened flow in vicinity of a river mouth is formed only if a river current is fast enough. At the same time, a freshened flow is abruptly decelerated by friction with ambient sea only if its kinetic energy, i.e., river discharge rate, is relatively low. Second, transformation of kinetic energy of a river flow to potential energy of a hydraulic jump depends on local salinity anomaly. Therefore, ambient sea salinity has to be high enough, which occurs in absence of intense freshwater accumulation in vicinity of a river mouth. Third, depth of a plume has to be smaller than sea depth near a river mouth. In this case, a river plume does not exhibit friction with sea bottom, which can hinder formation of a hydraulic jump.

Many small and rapid mountainous rivers that inflow to deep coastal sea areas correspond to the conditions listed above. These rivers have small but steep drainage basins that result in high flow velocities and small discharge rates. Steep coastal bathymetry typical for mountainous coasts provides quick renewal of sea water in vicinity of river mouths by coastal circulation. Discharges of such rivers form hydraulic jumps and generate internal waves in many world coastal regions (New Guinea, New Zealand, Mexico, Peru, Chile, Taiwan, etc.), which is regularly observed by satellite imagery. Moreover, many of these regions have regular flash flooding events on small rivers during rainfall [25, 30, 73]. The resulting simultaneous generation of high-frequency internal waves from multiple and closely spaced river mouths was registered in several of the mountainous regions listed above.

The processes of generation, propagation, and dissipation of internal waves described above induce transformation of river flow kinetic energy to turbulence in frontal zones of a river plume. As a result, these processes increase mixing in bottom and lateral boundaries of a plume and reduce freshwater volume accumulated in a river plume. This pattern of energy transform observed for small rivers of RCBS is significantly different from those that are typical for larger rivers and/or rivers with less rapid currents, which discharges form recirculating bulges in vicinity of river mouths instead of hydraulic jumps [9, 15, 56]. As a result, a kinetic energy of a river flow transforms to pressure gradient potential energy and kinetic energy of a bulge anticyclonic flow. In this case, increase in a kinetic energy of a

river flow increases freshwater accumulation rate within a bulge and decreases mixing between a river plume and ambient sea [9, 15]. Therefore, generation of internal waves is an important feature of river plumes formed by small and rapid rivers, which strongly affects their structure and dynamics.

5. Conclusions

In this chapter, we described specific features of structure and dynamics of small river plumes, which are significantly different from those typical for large plumes. Small river plumes are river plumes with small residence time of freshened water (hours and days), which mixing with ambient sea limitedly influences its salinity. Small plumes have sharp salinity gradients at their boundaries with ambient sea, which hinders vertical energy transfer between a small plume and subjacent sea. As a result, small plumes are mainly wind driven, while the role of circulation of ambient sea in their dynamics is negligible.

Small plumes are characterized by energetic temporal variability and inhomogeneous horizontal structure. Position, shape, and area of a small plume can significantly change during several hours in response to variability of wind forcing and river discharge rate. Small plumes have very small near-field part and do not form a recirculating bulge adjacent to river mouths due to efficient deceleration of inflowing river runoffs and quick decay of their initial inertia. The wind-induced Ekman transport within a small plume occurs at a wide range of angles to the wind direction during upwelling, onshore, and offshore wind-forcing periods with the largest values in the near-field part of a plume. Interaction between neighboring small plumes can strongly influence their structure and dynamics. Collision and coalescence of multiple small plumes in response to rain-induced flooding events results in the decrease of mixing intensity within small plumes and intensification of their alongshore spreading.

Finally, high-frequency internal waves are generated in certain small plumes formed by rivers with high flow velocity. Such a river inflows to coastal sea, abruptly decelerates, and forms a hydraulic jump in vicinity of a river mouth. Formation and relaxation of a hydraulic jump induces generation of high-frequency internal waves that propagate offshore. These internal waves strongly influence turbulence and mixing at a stratified layer between a buoyant river plume and subjacent ambient sea.

Acknowledgements

Conflict of interest

The authors declare that they have no conflict of interests.

Author details

Alexander Osadchiev* and Peter Zavialov
Shirshov Institute of Oceanology, Russian Academy of Sciences, Moscow, Russia

*Address all correspondence to: osadchiev@ocean.ru

IntechOpen

References

[1] Emmett RL, Krutzikowsky GK, Bentley P. Abundance and distribution of pelagic piscivorous fishes in the Columbia River plume during spring/early summer 1998–2003: Relationship to oceanographic conditions, forage fishes, and juvenile salmonids. Progress in Oceanography. 2006;**68**:1-26. DOI: 10.1016/j.pocean.2005.08.001

[2] Milliman JD, Lin SW, Kao SJ, Liu JP, Liu CS, Chiu JK, et al. Short-term changes in seafloor character due to flood-derived hyperpycnal discharge: Typhoon Mindulle, Taiwan, July 2004. Geology. 2007;**35**:779-782. DOI: 10.1130/G23760A.1

[3] Zhou MJ, Shen ZL, Yu RC. Responses of a coastal phytoplankton community to increased nutrient input from the Changjiang (Yangtze) River. Continental Shelf Research. 2008;**28**:1483-1489. DOI: 10.1016/j.csr.2007.02.009

[4] Huang WJ, Cai WJ, Wang Y, Lohrenz SE, Murrell MC. The carbon dioxide system on the Mississippi River-dominated continental shelf in the northern Gulf of Mexico: 1. Distribution and air-sea CO_2 flux. Journal of Geophysical Research, Oceans. 2015;**120**:1429-1445. DOI: 10.1002/2014jc010498

[5] Osadchiev AA, Izhitskiy AS, Zavialov PO, Kremenetskiy VV, Polukhin AA, Pelevin VV, et al. Structure of the buoyant plume formed by Ob and Yenisei River discharge in the southern part of the Kara Sea during summer and autumn. Journal of Geophysical Research, Oceans. 2017;**122**:5916-5935. DOI: 10.1002/2016JC012603

[6] Zavialov PO, Pelevin VV, Belyaev NA, Izhitskiy AS, Konovalov BV, Krementskiy VV, et al. High resolution LiDAR measurements reveal fine internal structure and variability of sediment-carrying coastal plume. Estuarine, Coastal and Shelf Science. 2018;**205**:40-45. DOI: 10.1016/j.ecss.2018.01.008

[7] O'Donnell J. The dynamics of estuary plumes and fronts. In: Valle-Levinson A, editor. Contemporary Issues in Estuarine Physics. Cambridge: Cambridge University Press; 2010. pp. 186-246

[8] Hetland RD, Hsu T-J. Freshwater and sediment dispersal in large river plumes. In: Bianchi TS, Allison MA, Cai W-J, editors. Biogeochemical Dynamics at Large River-Coastal Interfaces: Linkages with Global Climate Change. New York: Springer; 2013. pp. 55-85

[9] Horner-Devine AR, Hetland RD, MacDonald DG. Mixing and transport in coastal river plumes. Annual Review of Fluid Mechanics. 2015;**47**:569-594. DOI: 10.1146/annurev-fluid-010313-141408

[10] Chao SY, Boicort WG. Onset of estuarine plumes. Journal of Physical Oceanography. 1986;**16**:2137-2149. DOI: 10.1175/1520–0485(1986)016<2137:OOEP>2.0.CO;2

[11] Simpson JH. Physical processes in the ROFI regime. Journal of Marine Systems. 1997;**12**:3-15. DOI: 10.1016/s0924-7963(96)00085-1

[12] Horner-Devine AR, Fong DA, Monismith SG, Maxworthy T. Laboratory experiments simulating a coastal river discharge. Journal of Fluid Mechanics. 2006;**555**:203-232. DOI: 10.1017/s0022112006008937

[13] Warrick JA, Farnsworth KL. Coastal river plumes: Collisions and coalescence. Progress in Oceanography. 2017;**151**:245-260. DOI: 10.1016/j.pocean.2016.11.008

[14] O'Donnell J. The formation and fate of a river plume: A numerical model. Journal of Physical Oceanography. 1990; **20**:551-569. DOI: 10.1175/1520-0485 (1990)020<0551:TFAFOA>2.0.CO;2

[15] Fong DA, Geyer WR. Response of a river plume during an upwelling favorable wind event. Journal of Geophysical Research. 2001;**106**: 1067-1084. DOI: 10.1029/2000jc900134

[16] Fong DA, Geyer WR. The alongshore transport of freshwater in a surface-trapped river plume. Journal of Physical Oceanography. 2002;**32**: 957-972. DOI: 10.1175/1520-0485(2002) 032<0957:tatofi>2.0.co;2

[17] Avicola G, Huq P. The characteristics of the recirculating bulge region in coastal buoyant outflows. Journal of Marine Research. 2003;**61**:435-463. DOI: 10.1357/ 002224003322384889

[18] Yankovsky AE, Hickey BM, Munchow AK. Impact of variable inflow on the dynamics of a coastal buoyant plume. Journal of Geophysical Research, Oceans. 2001;**106**:19809-19824. DOI: 10.1029/2001jc000792

[19] Whitney MM, Garvine RW. Wind influence on a coastal buoyant outflow. Journal of Geophysical Research. 2005;**110**:C03014. DOI: 10.1029/ 2003jc002261

[20] Korotenko KA, Osadchiev AA, Zavialov PO, Kao R-C, Ding C-F. Effects of bottom topography on dynamics of river discharges in tidal regions: Case study of twin plumes in Taiwan Strait. Ocean Science. 2014;**10**:865-879. DOI: 10.5194/os-10-863-2014

[21] Yuan Y, Horner-Devine AR, Avener M, Bevan S. The role of periodically varying discharge on river plume structure and transport. Continental Shelf Research. 2018;**158**:15-25. DOI: 10.1016/j.csr.2018.02.009

[22] Geyer WR, Hill P, Milligan T, Traykovski P. The structure of the Eel River plume during floods. Continental Shelf Research. 2000;**20**:2067-2093. DOI: 10.1016/S0278-4343(00)00063-7

[23] Thomas A, Weatherbee RA. Satellite-measured temporal variability of the Columbia River plume. Remote Sensing of Environment. 2006;**100**: 167-178. DOI: 10.1016/j.rse.2005.10.018

[24] Ostrander CE, McManus MA, DeCarlo EH, Mackenzie FT. Temporal and spatial variability of freshwater plumes in a semi-enclosed estuarine–bay system. Estuaries and Coasts. 2008; **31**:192-203. DOI: 10.1007/s12237-007-9001-z

[25] Osadchiev A, Korshenko E. Small river plumes off the northeastern coast of the Black Sea under average climatic and flooding discharge conditions. Ocean Science. 2017;**13**:465-482. DOI: 10.5194/os-13-465-2017

[26] Vorosmarty C, Askew A, Grabs W, Barry RG, Birkett C, Doll P, et al. Global water data: A newly endangered species. Eos, Transactions of the American Geophysical Union. 2001;**82**:54-58. DOI: 10.1029/01eo00031

[27] Hrachowitz M, Savenije HHG, Bloschl G, McDonnelld JJ, Sivapalan M, Pomeroyg JW, et al. A decade of predictions in ungauged basins (PUB)—A review. Hydrological Sciences Journal. 2013;**58**:1198-1255. DOI: 10.1080/ 02626667.2013.803183

[28] Milliman JD, Syvitski JPM. Geomorphic-tectonic control of sediment discharge to the ocean: The importance of small mountainous rivers. Journal of Geology. 1992;**100**:525-544. DOI: 10.1086/629606

[29] Milliman JD, Farnsworth KL, Albertin CS. Flux and fate of fluvial sediments leaving large islands in the East Indies. Journal of Sea Research.

1999;**41**:97-107. DOI: 10.1016/ s1385-1101(98)00040-9

[30] Mertes LAK, Warrick JA. Measuring flood output from 110 coastal watersheds in California with field measurements and SeaWiFS. Geology. 2001;**29**:659-662. DOI: 10.1130/ 0091-7613(2001)029<0659: mfofcw>2.0.co;2

[31] Wheatcroft RA, Goni MA, Hatten JA, Pasternack GB, Warrick JA. The role of effective discharge in the ocean delivery of particulate organic carbon by small, mountainous river systems. Limnology and Oceanography. 2010;**55**: 161-171. DOI: 10.4319/lo.2010.55.1.0161

[32] Kniskern TA, Warrick JA, Farnsworth KL, Wheatcroft RA, Goni MA. Coherence of river and ocean conditions along the US West Coast during storms. Continental Shelf Research. 2011;**31**:789-805. DOI: 10.1016/j.csr.2011.01.012

[33] Saldias GS, Largier JL, Mendes R, Perez-Santos I, Vargas CA, Sobarzo M. Satellite-measured interannual variability of turbid river plumes off central-southern Chile: Spatial patterns and the influence of climate variability. Progress in Oceanography. 2016;**146**: 212-222. DOI: 10.1016/j.pocean. 2016.07.007

[34] Meybeck M, Laroche L, Durr HH, Syvitski JPM. Global variability of daily total suspended solids and their fluxes in rivers. Global and Planetary Change. 2003;**39**:65-93. DOI: 10.1016/s0921-8181 (03)00018-3

[35] Brodie J, Schroeder T, Rohde K, Faithful J, Masters B, Dekker A, et al. Dispersal of suspended sediments and nutrients in the Great Barrier Reef lagoon during river-discharge events: Conclusions from satellite remote sensing and concurrent flood-plume sampling. Marine and Freshwater Resources. 2010;**61**:651-664. DOI: 10.1071/MF08030

[36] Hilton RG, Galy A, Hovius N, Horng M-J, Chen H. Efficient transport of fossil organic carbon to the ocean by steep mountain rivers: An orogenic carbon sequestration mechanism. Geology. 2011;**39**:71-74. DOI: 10.1130/ g31352.1

[37] Bao H, Lee TY, Huang JC, Feng X, Dai M, Kao SJ. Importance of oceanian small mountainous rivers (SMRs) in global land-to-ocean output of lignin and modern biospheric carbon. Scientific Reports. 2015;**5**:16217. DOI: 10.1038/srep16217

[38] Romero L, Siegel DA, McWilliams JC, Uchiyama Y, Jones C. Characterizing storm water dispersion and dilution from small coastal streams. Journal of Geophysical Research, Oceans. 2016; **121**:3926-3943. DOI: 10.1002/ 2015JC011323

[39] Geyer WR, Beardsley RC, Lentz SJ, Candela J, Limeburner R, Johns WE, et al. Physical oceanography of the Amazon shelf. Continental Shelf Research. 1996;**16**:575-616. DOI: 10.1016/0278-4343(95)00051-8

[40] Schiller RV, Kourafalou VH, Hogan P, Walker ND. The dynamics of the Mississippi River plume: Impact of topography, wind and offshore forcing on the fate of plume waters. Journal of Geophysical Research, Oceans. 2011; **116**:C06029. DOI: 10.1029/ 2010JC006883

[41] Denamiel C, Budgell WP, Toumi R. The Congo River plume: Impact of the forcing on the far-field and near-field dynamics. Journal of Geophysical Research, Oceans. 2013;**118**:964-989. DOI: 10.1002/jgrc.20062

[42] Korotkina OA, Zavialov PO, Osadchiev AA. Submesoscale variability of the current and wind fields in the

coastal region of Sochi. Oceanology. 2011;**51**:745-754. DOI: 10.1134/ s0001437011050109

[43] Korotkina OA, Zavialov PO, Osadchiev AA. Synoptic variability of currents in the coastal waters of Sochi. Oceanology. 2014;**54**:545-556. DOI: 10.1134/s0001437014040079

[44] Osadchiev AA, Zavialov PO. Lagrangian model of a surface-advected river plume. Continental Shelf Research. 2013;**58**:96-106. DOI: 10.1016/j. csr.2013.03.010

[45] Zavialov PO, Makkaveev PN, Konovalov BV, Osadchiev AA, Khlebopashev PV, Pelevin VV, et al. Hydrophysical and hydrochemical characteristics of the sea areas adjacent to the estuaries of small rivers if the Russian coast of the Black Sea. Oceanology. 2014;**54**:265-280. DOI: 10.1134/s0001437014030151

[46] Osadchiev AA. A method for quantifying freshwater discharge rates from satellite observations and Lagrangian numerical modeling of river plumes. Environmental Research Letters. 2015;**10**:085009. DOI: 10.1088/ 1748-9326/10/8/085009

[47] Osadchiev AA. Estimation of river discharge based on remote sensing of a river plume. Proceedings of SPIE. 2015; **9638**:96380H. DOI: 10.1117/12.2192672

[48] Osadchiev AA, Korotenko KA, Zavialov PO, Chiang W-S, Liu C-C. Transport and bottom accumulation of fine river sediments under typhoon conditions and associated submarine landslides: Case study of the Peinan River, Taiwan. Natural Hazards and Earth System Sciences. 2016;**16**:51-54. DOI: 10.5194/nhess-16-41-2016

[49] Ross ON, Sharples J. Recipe for 1-D Lagrangian particle tracking models in space-varying diffusivity. Limnology and Oceanography: Methods. 2004;**2**: 289-302. DOI: 10.4319/lom.2004.2.289

[50] Smagorinsky J. General circulation experiments with the primitive equation. 1. The basic experiment. Monthly Weather Review. 1963;**91**: 99-165. DOI: 10.1175/1520-0493(1963) 091<0099:GCEWTP>2.3.CO;2

[51] Large WG, McWilliams JC, Doney SC. Oceanic vertical mixing: A review and a model with a nonlocal boundary layer parameterization. Reviews of Geophysics. 1994;**32**:363-403. DOI: 10.1029/94RG01872

[52] Jaoshvili S. The rivers of the Black Sea. In: Chomeriki I, Gigineishvili G, Kordzadze A, editors. European Environmental Agency, Technical Report No. 71. 2002. Available from: h ttps://www.eea.europa.eu/publications/ technical_report_2002_71/at_download/ file [Accessed: 15 April 2019]

[53] Osadchiev AA, Sedakov RO. Spreading dynamics of small river plumes off the northeastern coast of the Black Sea observed by Landsat 8 and Sentinel-2. Remote Sensing of Environment. 2019;**221**:522-533. DOI: 10.1016/j.rse.2018.11.043

[54] Yankovsky AE, Chapman DC. A simple theory for the fate of buoyant coastal discharges. Journal of Physical Oceanography. 1997;**27**:1386-1401. DOI: 10.1175/1520-0485(1997)027<1386: astftf>2.0.co;2

[55] Nof D, Pichevin T. The ballooning of outflows. Journal of Physical Oceanography. 2001;**31**:3045-3058. DOI: 10.1175/1520-0485(2001)031< 3045:tboo>2.0.co;2

[56] MacDonald DG, Goodman L, Hetland RD. Turbulent dissipation in a near-field river plume: A comparison of control volume and microstructure with a numerical model. Journal of Geophysical Research. 2007;**112**: C07026. DOI: 10.1029/2006JC004075

[57] Chant RJ, Wilkin J, Zhang W, Choi B-J, Hunter E, Castelao R, et al.

Dispersal of the Hudson River plume in the New York Bight: Synthesis of observational and numerical studies during LaTTE. Oceanography. 2008; **21**:148-161. DOI: 10.5670/oceanog. 2008.11

[58] Liu Y, MacCready P, Hickey BM, Dever EP, Kosro PM, Banas NS. Evaluation of a coastal ocean circulation model for the Columbia River plume in summer 2004. Journal of Geophysical Research. 2009;**114**:C00B04. DOI: 10.1029/2008gl036447

[59] Bourrin F, Friend PL, Amos CL, Manca E, Ulses C, Palanques A, et al. Sediment dispersal from a typical Mediterranean flood: The Têt River, Gulf of Lions. Continental Shelf Research. 2008;**28**:1895-1910. DOI: 10.1016/j.csr.2008.06.005

[60] Zhao J, Gong W, Shen J. The effect of wind on the dispersal of a tropical small river plume. Frontiers of Earth Science. 2018;**12**:170-190. DOI: 10.1007/ s11707-016-0628-6

[61] Zhurbas NV. The wind-induced drift velocity of the freshwater layer on the sea's surface. Oceanology. 2013;**53**:136-144. DOI: 10.1134/ s0001437013020161

[62] Choi BJ, Wilkin JL. The effect of wind on the dispersal of the Hudson River plume. Journal of Physical Oceanography. 2007;**37**:1878-1897. DOI: 10.1175/JPO3081.1, 2007

[63] Xia M, Xie L, Pietrafesa LJ. Modeling of the Cape Fear River estuary plume. Estuaries and Coasts. 2007;**30**:698-709. DOI: 10.1007/ BF02841966

[64] Xia M, Xie L, Pietrafesa LJ, Whitney MM. The ideal response of a Gulf of Mexico estuary plume to wind forcing: Its connection with salt flux and a Lagrangian view. Journal of Geophysical Research, Oceans. 2011;**116**:C08035. DOI: 10.1029/2010JC006689

[65] Jurisa JT, Chant R. The coupled Hudson River estuarine-plume response to variable wind and river forcings. Ocean Dynamics. 2012;**62**:771-784. DOI: 10.1007/s10236-012-0527-7

[66] Rennie SE, Largier JL, Lentz SJ. Observations of a pulsed buoyancy current downstream of Chesapeake Bay. Journal of Geophysical Research. 1999; **104**:18227-18240. DOI: 10.1029/ 1999JC900153

[67] Pullen JD, Allen JS. Modeling studies of the coastal circulation off northern California: Shelf response to a major Eel River flood event. Continental Shelf Research. 2000;**20**:2213-2238. DOI: 10.1016/S0278-4343(00)00068-6

[68] Johnson D, Weidemann A, Arnone R, Davis C. Chesapeake Bay outflow plume and coastal upwelling events: Physical and optical properties. Journal of Geophysical Research. 2001;**106**: 11613-11622. DOI: 10.1029/ 1999JC000185

[69] Alexeevsky NI, Magritsky DV, Koltermann KP, Krylenko IN, Toropov PA. Causes and systematics of inundations of the Krasnodar territory on the Russian Black Sea coast. Natural Hazards and Earth System Sciences. 2016;**16**:1289-1308. DOI: 10.5194/nhess-16-1289-2016

[70] Zalesny VB, Diansky NA, Fomin VV, Moshonkin SN, Demyshev SG. Numerical model of the circulation of the Black Sea and the Sea of Azov. Russian Journal of Numerical and Analytical Mathematical Modelling. 2012;**27**:95-112. DOI: 10.1515/rnam-2012-0006

[71] Zalesny VB, Gusev AV, Moshonkin SN. Numerical model of the hydrodynamics of the Black Sea and the Sea of Azov with variational initialization of temperature and salinity. Izvestiya Atmospheric and Oceanic Physics. 2013;**49**:642-658. DOI: 10.1134/S0001433813060133

[72] Osadchiev AA. Small mountainous rivers generate high-frequency internal waves in coastal ocean. Scientific Reports. 2018;**8**:16609. DOI: 10.1038/s41598-018-35070-7

[73] Nezlin NP, DiGiacomo PM, Stein ED, Ackerman D. Stormwater runoff plumes observed by SeaWiFS radiometer in the Southern California Bight. Remote Sensing of Environment. 2005;**98**:494-510. DOI: 10.1016/j.rse.2005.08.008